WIND MEASUREMENTS WITH THE ALOMAR RMR-LIDAR: METHOD DESCRIPTION AND INITIAL RESULTS

Jens Hildebrand, Gerd Baumgarten, Jens Fiedler, and Franz-Josef Lübken

Leibniz-Institut für Atmosphärenphysik,
Schlossstraße 6, 18209 Kühlungsborn, Germany; E-mail: hildebrand@iap-kborn.de

ABSTRACT

In this paper we present a new method to measure winds in the middle atmosphere by the Rayleigh/Mie/Raman lidar at ALOMAR (Arctic Lidar Observatory for Middle Atmosphere Research). The so called Doppler Rayleigh Iodine System is based on the detection of Doppler shift of light backscattered from molecules moving with the wind. Since this Doppler shift is very small, sophisticated laser and detection control is required. We present details how crucial system parameters are taken into account when deriving winds. Measurements performed in January 2009 show good agreement with ECMWF in the height range of overlapping data. The measurements were analyzed in an altitude range of 28 km to 80 km allowing for an measurement uncertainty of less than ± 17 m/s.

1. INTRODUCTION

Wind measurements are fundamental for our understanding of the dynamical and thermal processes in the atmosphere [6]. Unfortunately, wind measurements in the altitude range between approximately 30 and 70 km are very difficult since this region is too high for balloons and it is located below the ionosphere, i. e., radars do not receive significant backscatter for determining winds. Rockets cover these regions, but they only allow sporadic soundings [7]. Satellites also fail to ensure reliable measurement in this height range. Our Rayleigh/Mie/Raman (RMR) lidar at the Arctic Lidar Observatory for Middle Atmosphere Research (ALOMAR) in Northern Norway (69° N, 16° E) routinely measures temperatures and aerosols in the stratosphere and mesosphere [9, 8, 2, 1]. Within the last years it has been modified to allow wind measurements as well.

The RMR-lidar employs a pair of injection-seeded Nd:YAG lasers, each with a total output of 150 MW peak power at the three emitted wavelengths 1064 nm, 532 nm, and 355 nm. Backscattered light is collected by two 1.8 m diameter telescopes which can be tilted up to 30° off-zenith. Moreover each telescope covers an azimuth range of 90° in such a way that one is able to access the north-to-west quadrant, the other one the south-to-east quadrant. Tilting the telescopes of the twin-lidar allows to measure wind in two different directions simultaneously. The ALOMAR RMR-lidar is capable to operate under all daylight conditions which is achieved by the small telescope field-of-view (180 µrad) and the application of actively stabilized Fabry-Pérot etalons.

For reliable statistics of atmospheric dynamics a routine measurement operation of the system is required. This is challenging as a spectral stability of better than 10^{-8} and/or a monitoring of the system performance is needed. We describe our approach of measuring relevant system parameters and taking those in the analysis into account.

2. THE DOPPLER RAYLEIGH IODINE SYSTEM

2.1. Algorithm

The frequency of light backscattered by atmospheric molecules is changed by Doppler effect. Two main effects have to be taken into account when deriving wind speeds by lidar: (1) the mean frequency is shifted due to Doppler shift at moving scatterers, and (2) broadening of backscattered light due to thermal motion of the molecules (Fig. 1). The mean frequency shift (1) is a direct measure of line of sight wind speed it is the quantity we want to derive. Wind speed of 1 m/s causes a frequency shift of -3.76 MHz, as depicted in the upper panel of Fig. 1 for 100 m/s along and against line of sight, respectively. The broadening of backscattered light due to thermal motion of the molecules (2) has to be taken into account. Although the system is designed to be least sensitive to atmospheric temperature changes, the large temperature range from more than 300 K during stratospheric warmings to less than 160 K in summer has to be taken into account. For temperatures between 175 and 325 K an increase in temperature of 1 K causes a Doppler broadening of about 4.7 MHz. Shown in lower panel of Fig. 1 are Cabannes lines for temperatures of 175, 250, and 325 K in green, blue, and purple, respectively.

Proc. '19th ESA Symposium on European Rocket and Balloon Programmes and Related Research, Bad Reichenhall, Germany, 7–11 June 2009 (ESA SP-671, September 2009)

Since the frequency shift is on the order of $\Delta\nu/\nu \sim 10^{-7}$–$10^{-8}$ only, a very sensitive frequency discriminator is needed. We use the steep edge of an absorption line of molecular iodine to transform the frequency shift to an easier to measure intensity change [e.g. 4]. This edge raises from minimal to maximal transmittance within $\frac{1}{10}$ of the line-width of the backscattered light. The resulting signal is proportional to the convolution of iodine spectrum and atmospheric signal, as illustrated as green area in Fig. 2; hence it is a function of Doppler shift.

Taking variations of atmospheric transmission into account we, use a second channel without iodine cell for reference. This channel is also used to calculate simultaneously temperature. Assuming hydrostatic equilibrium,

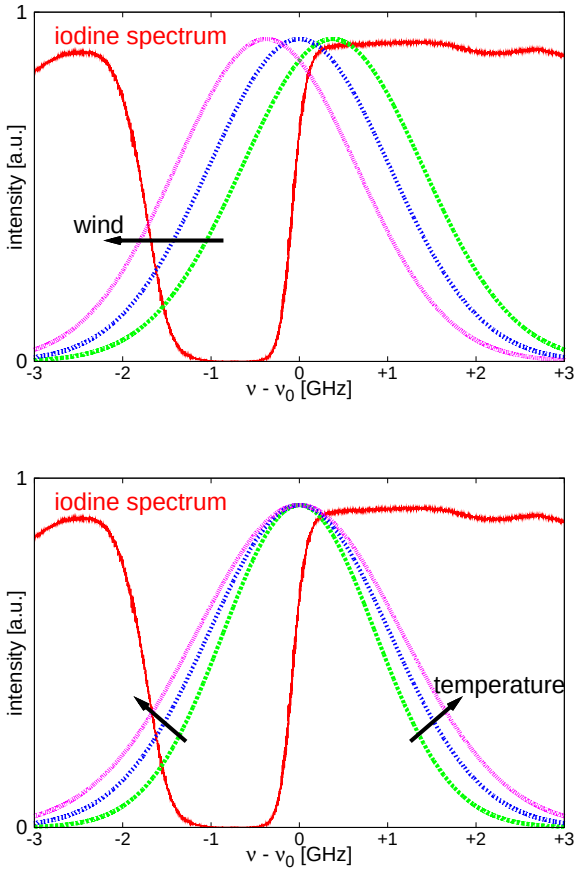

Figure 1. Influence of line of sight wind and temperature on light backscattered from moving molecules. The Cabannes line of the light backscattered from molecules is shown in comparison to the transmittance of the cell used in the detector bench. Upper panel: Doppler shift of the received Cabannes line due to wind. The blue line is for 0-wind and the green and purple correspond to $100\,m/s$ *along and against the line of sight, respectively. Lower panel: Doppler broadening of the Cabannes line for different temperatures (*$175\,K$ *– green,* $250\,K$ *– blue,* $325\,K$ *– purple).*

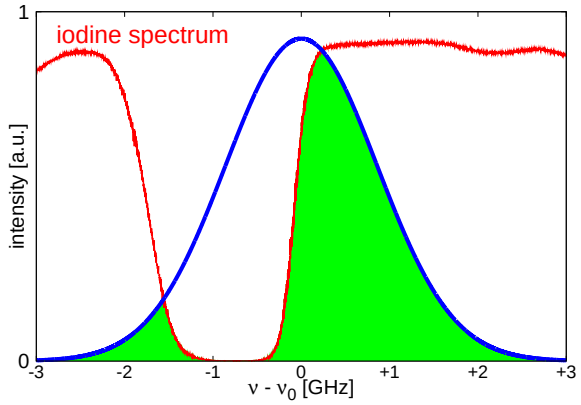

Figure 2. Like Fig. 1 but for a given combination of temperature and wind. The convolution of iodine spectrum and atmospheric signal is detected by the channel behind the iodine cell. The detected signal is proportional to the green area.

the relative density profile is converted to a height profile of the atmospheric temperature through integration [e.g. 5].

The ratio of both, the so called "Doppler ratio", depends strongly on wind speed and weakly on temperature. Fig. 3 shows a simulated Doppler ratio matrix which is used as lookup table for deriving wind speeds. Since the temperature is known from our measurements the Doppler ratio is a unique measure of wind speed. The spectrum of the iodine cell in the detection system is measured regularly using the narrow band seed laser.

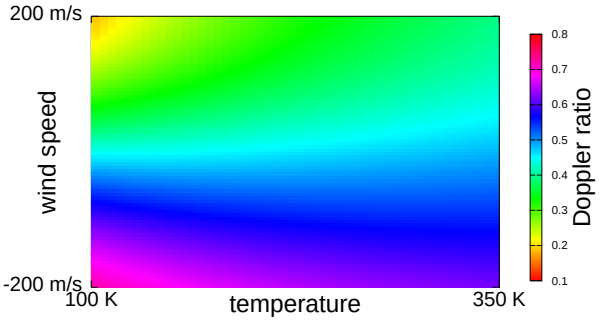

Figure 3. Simulated Doppler ratio as function of temperature and line of sight wind speed. Each point of the graph corresponds to the ratio of signal detected by the channel behind iodine cell (Fig. 2) and signal detected by the channel without iodine cell (not shown), both calculated for corresponding temperature and wind speed. The absolute value of the Doppler ratio depends on the optical components used in the system.

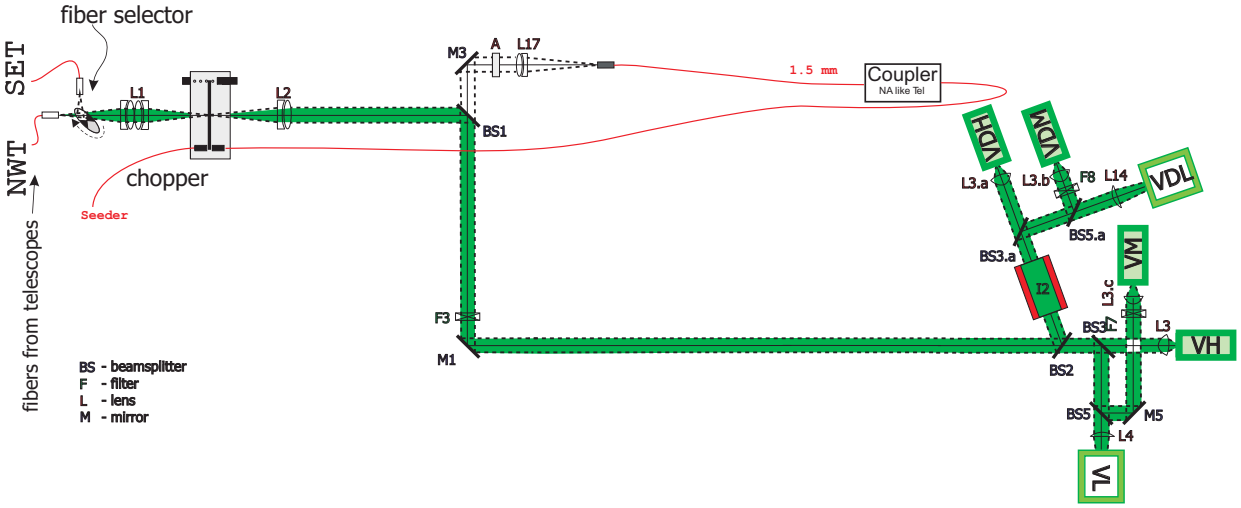

Figure 4. Layout of detection branch for 532 *nm. Atmospheric signal enters from left, is guided with mirrors through the detection system, is split and collected by six channels. The three detectors with different sensitivities allow to cover the large altitude range from* 15 *to* 100 *km. For daytime measurements a double etalon system is used. For normalization purposes light from the seed laser is coupled into the detection system about* 1 *ms after the laser has fired.*

2.2. Monitoring of Transmitted Frequency

For correct determination of Doppler shift it is essential to know the transmitted frequency. Therefore both transmitting lasers are injection-seeded by one single external seed laser whose frequency is stable to better than 6 MHz in 3 years [3]. This stability is achieved by locking the frequency of the seed laser to a certain point of the absorption edge of an iodine vapor cell. The quality and stability of the seeding process is important for the whole system performance. Inherently the method of cavity length matching used in pulsed lasers introduces a frequency dither. Additionally temperature changes, flash lamp aging and other processes may cause a frequency difference between seed and transmitting lasers.

Therefore we monitor the transmitted frequencies of both transmitting lasers on single pulse basis using a so-called "Laser Pulse Spectrometer". It consists basically of a fiber switch, a iodine vapor cell, and two fast photo diodes which are sampled with a digital oscilloscope. Alternately four fibers are coupled into the fiber switch: light from seed laser, light from each transmitting laser and an unassigned one for background correction. Afterward the light is split as follows: one part is directed through the iodine cell and detected by one of the photo diodes, the other one is detected directly. For each of the three lasers the ratio of detected voltages is derived. The duration of each measurement cycle is two minutes, 30 seconds for each fiber. Each logged data point represents 20 times the average of 4 laser pulses. For further analysis we average over the same time interval like the lidar raw data. Merging the ratio of one transmitting laser and the one of the seed laser allows to derive the frequency offset of this transmitting laser. This frequency offset is transformed into a offset in line of sight wind speed and has to be included in the wind retrieval.

2.3. Detection Branch

A simplified sketch of the detection branch for the 532 nm wavelength, which is used for wind measurements, is shown in Fig. 4.

Light from both telescopes is coupled into the optical bench by a segmented mirror which is synchronized to the laser pulses. For daytime measurements the light is guided through a double Fabry-Pérot etalon which can be bypassed for nighttime measurements. Light is then split in two parts. One part is detected directly by the reference channel, which also provides temperature measurement. The other part is guided through a sealed iodine vapor cell, which is operated at a constant temperature. Its transmittance strongly depends on frequency. Both Doppler and reference branch consist each of three detectors of different sensitivities to cover a high altitude range. The ratio of both channels gives the measured Doppler ratio. The efficiency of the photon counters has to be taken into account since it varies with temperature. Therefore light of the extremely stable seed laser is coupled into the branch after each pulse to normalize the measured Doppler ratio. This also corrects transmittance of used optics such as beamsplitters, lenses, and etalon.

3. FIRST RESULTS

Two exemplary profiles of temperature, zonal wind speed, and meridional wind speed measured with the ALOMAR RMR-lidar are shown in Fig. 5 for January 23rd 2009. End of January 2009 was influenced by a strong major stratospheric warming. Note the high temperature in stratosphere and low temperature in mesosphere.

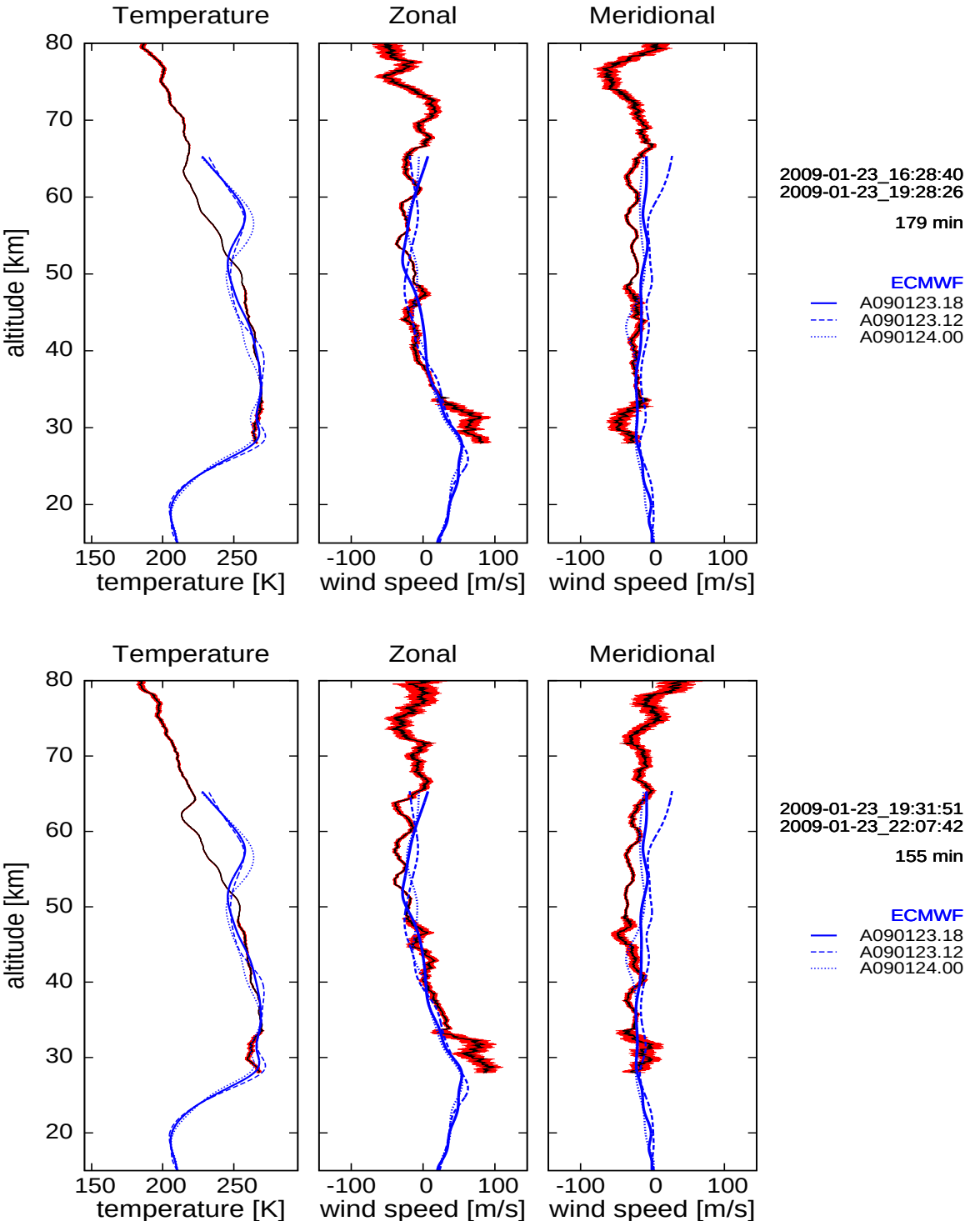

Figure 5. Temperature and wind profiles for January 23rd 2009 and comparison to ECMWF data at ALOMAR for three different times. The upper panel shows the measurements that were calibrated to ECMWF at 35 km altitude by adding a constant offset to the wind profile. The lower profiles show the following measurement with the same calibration factors.

The first profiles were integrated over three hours, from 16:28 till 19:28 UT. The measured power laser offset and Doppler ratio normalization is listed in Tab. 1. Also listed is a further calibration factor, corresponding to a wind offset, to normalize measured wind profile to ECMWF Model in the altitude range 30–40 km. This normalization is weighted with measurement uncertainty and values with too large errors are ignored. As it can be seen in the upper panel of Fig. 5 the wind shear in zonal wind of about 40 m/s between 35 and 55 km altitude is clearly visible both in modeled and in measured data. The increasing wind speed in higher altitudes fits also well for measured and modeled data. Meridional wind speed shows nearly no change in altitude, neither modeled nor calculated data. The second profiles (19:31–22:07 UT) were integrated over two and a half hours. The same calibration as for the previous measurement was used but changes in laser frequency and channel efficiency were taken into account, see Tab. 1. The lower panel of Fig. 5 shows that measured and modeled data compare very well. This shows that measured calibration factors are sufficient and no further calibration is needed in this example.

Table 1. Parameters for wind retrieval. Frequency offset of both transmitting lasers (referred to as L1 and L2) relative to seed laser, normalization factor of Doppler ratio (DR), and calibration factors of Doppler ratio to normalize to modeled wind speeds are listed. Laser 1 is assigned to the north-west telescope and provides meridional wind speed, while laser 2 is assigned to the south-east telescope providing zonal wind speed. Although frequency offset and normalization of Doppler ratio have changed, same calibration to ECMWF model is valid.

Time at 01. 23. 2009	16:28–19:28	19:31–22:07
frequency offset L1	-7.41 MHz	-3.29 MHz
frequency offset L2	-17.7 MHz	-14.6 MHz
norm. of DR L1	0.8897	0.8904
norm. of DR L2	0.8897	0.8902
calibration for DR L1	1.78	1.78
calibration for DR L2	2.05	2.05

4. SUMMARY

The first analysis of Doppler wind measurements with the ALOMAR RMR-lidar using a new analysis method was performed. The method takes several crucial system parameters into account when deriving wind speeds. Since January 2008 more than 500 hours of vector wind measurements were performed and about 70 hours of atmospheric calibration. The presented first results show very good comparison with modeled data.

ACKNOWLEDGMENTS

We gratefully acknowledge the support of the ALOMAR staff in running the RMR-lidar. The DoRIS project is funded by Deutsche Forschungsgemeinschaft (BA 2834/1-1).

REFERENCES

[1] Baumgarten, G., Fiedler, J., Lübken, F. J., & von Cossart, G. 2008, Journal of Geophysical Research (Atmospheres), 113, 6203

[2] Fiedler, J., Baumgarten, G., & Lübken, F.-J. 2009, J. Atmos. Solar-Terr. Phys., 424

[3] Fiedler, J., Baumgarten, G., & von Cossart, G. 2008, in Reviewed and revised papers presented at the 24th International Laser Radar Conference, 824–827

[4] Friedman, J. S., Tepley, C. A., Castleberg, P. A., & Roe, H. 1997, Opt. Lett., 22, 1648

[5] Kent, G. S. & Wright, R. W. H. 1970, Journal of Atmospheric and Terrestrial Physics, 32, 917

[6] Meriwether, J. W. & Gerrard, A. J. 2004, Reviews of Geophysics, 42, 3003

[7] Müllemann, A. & Lübken, F.-J. 2005, Adv. Space Res., 35(11), 1890

[8] Schöch, A., Baumgarten, G., & Fiedler, J. 2008, Ann. Geophys., 26, 1681

[9] von Zahn, U., von Cossart, G., Fiedler, J., et al. 2000, Ann. Geophys., 18, 815